On the required shape corrections to the local density and generalized gradient approximations to the Kohn-Sham potentials for molecular response calculations of (hyper)polarizabilities and excitation energies

Gruning, M.; Gritsenko, O.V.; van Gisbergen, S.J.A.; Baerends, E.J.

published in
Journal of Chemical Physics
2002

DOI (link to publisher)
10.1063/1.1476007

document version
Publisher's PDF, also known as Version of record

On the required shape corrections to the local density and generalized gradient approximations to the Kohn–Sham potentials for molecular response calculations of (hyper)polarizabilities and excitation energies

Myrta Grüning, Oleg V. Gritsenko, Stan J. A. van Gisbergen, and Evert Jan Baerends
Afdeling Theoretische Chemie, Vrije Universiteit, De Boelelaan 1083, 1081 HV Amsterdam, The Netherlands

(Received 10 January 2002; accepted 13 March 2002)

It is well known that shape corrections have to be applied to the local-density (LDA) and generalized gradient (GGA) approximations to the Kohn–Sham exchange–correlation potential in order to obtain reliable response properties in time dependent density functional theory calculations. Here we demonstrate that it is an oversimplified view that these shape corrections concern primarily the asymptotic part of the potential, and that they affect only Rydberg type transitions. The performance is assessed of two shape-corrected Kohn–Sham potentials, the gradient-regulated asymptotic connection procedure applied to the Becke–Perdew potential (BP–GRAC) and the statistical averaging of (model) orbital potentials (SAOP), versus LDA and GGA potentials, in molecular response calculations of the static average polarizability α, the Cauchy coefficient S_{-4}, and the static average hyperpolarizability β. The nature of the distortions of the LDA/GGA potentials is highlighted and it is shown that they introduce many spurious excited states at too low energy which may mix with valence excited states, resulting in wrong excited state compositions. They also lead to wrong oscillator strengths and thus to a wrong spectral structure of properties like the polarizability. LDA, Becke–Lee–Yang–Parr (BLYP), and Becke–Perdew (BP) characteristically underestimate contributions to α and S_{-4} from bound Rydberg-type states and overestimate those from the continuum. Cancellation of the errors in these contributions occasionally produces fortuitously good results. The distortions of the LDA, BLYP, and BP spectra are related to the deficiencies of the LDA/GGA potentials in both the bulk and outer molecular regions. In contrast, both SAOP and BP-GRAC potentials produce high quality polarizabilities for 21 molecules and also reliable Cauchy moments and hyperpolarizabilities for the selected molecules. The analysis for the N_2 molecule shows, that both SAOP and BP–GRAC yield reliable energies ω_i and oscillator strengths f_i of individual excitations, so that they reproduce well the spectral structure of α and S_{-4}. © *2002 American Institute of Physics.* [DOI: 10.1063/1.1476007]

I. INTRODUCTION

The importance of shape corrections to the LDA/GGA Kohn–Sham (KS) potentials, consisting of asymptotic correction to yield $-1/r$ behavior, as well as correction in the bulk molecular region, to set, e.g., the HOMO level at the first IP, for the calculation of response properties has been recognized[1] and has been demonstrated with various novel model exchange–correlation (xc) potentials for the (frequency dependent) dipole and quadrupole polarizabilities in Ref. 2, and for a range of response properties including excitation energies in Refs. 3–8. A common feature of the successful new potentials is their effectively more attractive character [with respect to the long-range asymptotics $v_{xc}(\infty)$] in the bulk and outer valence regions compared to the standard potentials of the local density approximation (LDA) and generalized gradient approximations (GGAs). This feature is illustrated with Fig. 1 where the xc potentials constructed by statistical averaging of (model) orbital potentials (SAOP)[7,9,10] and by gradient-regulated asymptotic connection procedure[8] applied to the GGA Becke–Perdew xc potential[11,12] (BP–GRAC) are plotted along the main axis of the molecule N_2. They are compared with the LDA potential and with the uncorrected BP potential. Both SAOP and BP–GRAC potentials are shifted downward in the bulk valence region by (roughly) a constant compared to the LDA and BP ones. Note, that in the BP–GRAC case this shift is explicitly introduced in the GRAC procedure (see the next section for the methodical details). In the outer region both SAOP and BP–GRAC potentials have the Coulombic asymptotics $-1/r$, while the LDA potential decays exponentially and the BP potential decays as $-c/r^2$.

These features of the new potentials bring a substantial improvement compared to the standard approximations of the energy gaps $\Delta\varepsilon_{ia}=\varepsilon_a-\varepsilon_i$ between the occupied valence ψ_i and the unoccupied ψ_a KS orbitals. The correct Coulombic asymptotics of the improved potentials leads to a relative stabilization of bound Rydberg-type states compared to the LDA/GGA potentials. This stabilization is however smaller than the downshift of the occupied orbitals due to the downshift of the SAOP and BP–GRAC potentials in the molecular region. Therefore, for higher-lying bound unoccupied Rydberg-type orbitals ψ_a the energy differences $\Delta\varepsilon_{ia}$ are substantially increased. This is important for the excitation spectra calculated with TDDFT, since $\Delta\varepsilon_{ia}$ serve in this theory as the zero order estimates of excitation energies. In addition, the correct Coulombic asymptotics of the improved potentials leads to an improved spatial extent of bound Rydberg-type states, which will affect the transition dipole

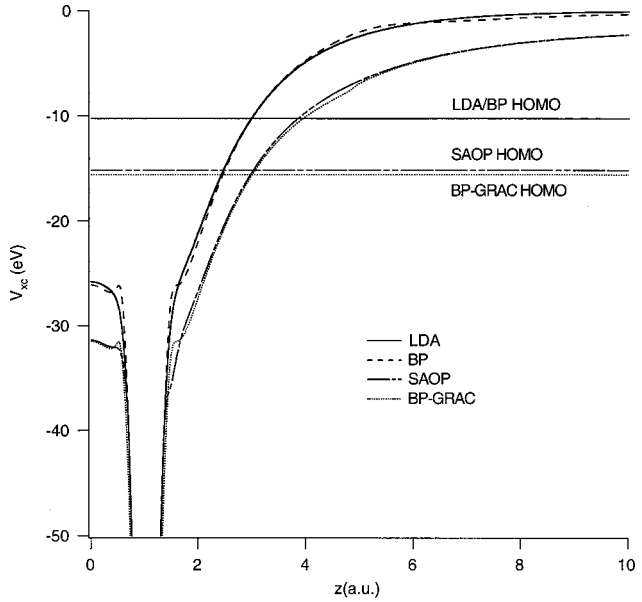

FIG. 1. The SAOP and BP–GRAC xc potentials are plotted along the main axis for the N_2 molecule. LDA and BP xc potentials are also plotted for comparison.

matrix elements. We stress that the new potentials, as well as the older van Leeuwen–Baerends one,[1] are not only asymptotically corrected, but the shape correction in the molecular region is at least as important. If the unoccupied orbital ψ_a is a low-lying one which has its amplitude mostly in the same region as the HOMO, it will be downshifted by about the same amount, so we do not expect a large change in the excitation energies to such an orbital. These effects of the new potentials appear to be essential (see the analysis in Sec. IV) for the correct description of both the excitation energies and of other characteristics of the excitations such as their composition in terms of contributing orbital excitations and their relative contributions to the calculated polarizabilities.

Both SAOP and GRAC potentials have been tested successfully in TDDFT calculations of excitation spectra of small prototype systems and they have been also applied to more complex systems. Recently, for example, the SAOP potential has been applied successfully to calculation of excitation spectra of transition metal tetrapyrroles and of zinc phthalocyanine,[13,14] and to calculation of polarizability and absorption spectra of alkali metal clusters.[15] Reliable results have been obtained with the BP–GRAC potential for the response properties of furan homologues.[16] These results corroborate the conclusion[5,17] that the calculated response properties of compact systems depends mainly on the quality of the approximate xc potential v_{xc} and they do not depend strongly on the approximation for the xc kernels f_{xc} describing the spatial change and time evolution of v_{xc} in response to a changing external potential. This allows to approximate f_{xc} with the static derivatives of the LDA (adiabatic LDA, ALDA) or GGA potentials, thus neglecting the frequency dependence and the spatial nonlocality of these kernels.

In this paper the performance of the SAOP and BP–GRAC potentials is assessed in TDDFT calculations of the static average polarizability α of 21 light molecules and also in calculations of the related properties such as the anisotropy of α, the Cauchy coefficient S_{-4} and the hyperpolarizability β. In Sec. II the methodical and computational details are given. In Sec. III the results of the SAOP and BP–GRAC molecular response calculations are compared with those of LDA and GGAs (BP and Becke–Lee–Yang–Parr (BLYP)[11,18] approximations) as well as with the experimental data. SAOP, BP–GRAC, and BP yield polarizabilities of a similar good quality and they substantially improve upon LDA and BLYP. Furthermore, SAOP and BP–GRAC perform definitely better than either BP or LDA and BLYP in calculation of the S_{-4} Cauchy coefficients and, especially, in calculation of the hyperpolarizabilities β. In Sec. IV the analysis of contributions from individual excitations to α and S_{-4} is performed for the case of the N_2 molecule, for which the corresponding experimental data are available. While SAOP and BP–GRAC reproduce very well the spectral structure of α and S_{-4}, LDA, BLYP, and BP considerably distort it, so that a good quality of the total BP α values appears to be the result of an error cancellation. The distortions of the LDA/GGA spectra are related to the deficient form of the corresponding potentials in both bulk and outer regions. Finally, conclusions are drawn in Sec. V.

II. COMPUTATIONAL DETAILS

The SAOP xc potential $v_{\mathrm{xc}}^{\mathrm{SAOP}}$ is constructed according to Refs. 7, 9, and 10 as the statistical average over the occupied KS orbitals ψ_i,

$$v_{\mathrm{xc}}^{\mathrm{SAOP}}(\mathbf{r})=\sum_{i=1}^{N} v_{\mathrm{xci}}^{\mathrm{mod}}(\mathbf{r})\frac{|\psi_i(\mathbf{r})|^2}{\rho(\mathbf{r})}, \tag{2.1}$$

of the model orbital potentials $v_{\mathrm{xci}}^{\mathrm{mod}}$. The latter are obtained with the interpolation

$$v_{\mathrm{xci}}^{\mathrm{mod}}(\mathbf{r})=e^{-2(\Delta\varepsilon_{iN})^2}v_{\mathrm{xc}}^{\mathrm{LB}\alpha}(\mathbf{r})+[1-e^{-2(\Delta\varepsilon_{iN})^2}]v_{\mathrm{xc}}^{\mathrm{GLLB}}(\mathbf{r}), \tag{2.2}$$

between the modified potential $v_{\mathrm{xc}}^{\mathrm{LB}\alpha}$ of van Leeuwen and Baerends (LB),[1] which has the proper Coulombic asymptotics $-1/r$, and the potential $v_{\mathrm{xc}}^{\mathrm{GLLB}}$ of Gritsenko, van Leeuwen, van Lenthe, and Baerends (GLLB),[19] which correctly reproduces the atomic shell structure in the inner regions. With, (2.1), (2.2) $v_{\mathrm{xc}}^{\mathrm{SAOP}}$ provides a balanced approximation to the KS potential v_{xc} in all regions.

The BP–GRAC potential $v_{\mathrm{xc}}^{\mathrm{BP-GRAC}}$ is obtained according to Ref. 8 with a seamless connection

$$v_{\mathrm{xc}}^{\mathrm{BP-GRAC}}(\mathbf{r})=[1-f(x)]v_{\mathrm{xc}}^{\mathrm{BP}}(\mathbf{r}) + f(x)[v_{\mathrm{xc}}^{\mathrm{LB}}(\mathbf{r})+(I_p+\varepsilon_N)] \tag{2.3}$$

between the BP potential $v_{\mathrm{xc}}^{\mathrm{BP}}$ in the bulk region and the LB potential $v_{\mathrm{xc}}^{\mathrm{LB}}$ at the asymptotics, the latter being shifted upward by the constant $(I_p+\varepsilon_N)$ where I_p is the first vertical ionization potential (VIP). In (2.3) $f(x)$ is the gradient-dependent interpolation function

$$f[x(\mathbf{r})]=\frac{1}{1+e^{-a[x(\mathbf{r})-b]}}, \tag{2.4}$$

TABLE I. First ionization potential: for BP–GRAC the experimental value (expt.) given as input, for SAOP and BP, respectively, $-\varepsilon_N^{\mathrm{SAOP}}$ and $-\varepsilon_N^{\mathrm{BP}}$; err. is the difference between SAOP/BP and GRAC (experimental) values.

	SAOP	Err.	BP	Err.	BLYP	Err.	LDA	Err.	Expt.
CS_2	10.72	0.65	6.86	−3.21	6.58	−3.49	6.89	−3.18	10.07
H_2S	10.25	−0.21	6.37	−4.09	6.12	−4.34	6.36	−4.1	10.46
C_2H_4	10.94	0.43	6.78	−3.73	6.53	−3.98	6.9	−3.61	10.51
PH_3	10.53	−0.06	6.78	−3.09	6.56	−3.31	6.73	−3.14	10.59
NH_3	10.7	−0.1	6.26	−4.54	6.08	−4.72	6.25	−4.55	10.8
OCS	11.76	0.58	7.54	−3.64	7.28	−3.9	7.6	−3.58	11.18
Cl_2	11.65	0.17	7.37	−4.11	7.15	−4.33	7.4	−4.08	11.48
C_2H_6	12.52	0.52	8.22	−3.78	8.06	−3.94	8.11	−3.89	12
SiH_4	12.49	0.19	8.63	−3.67	8.44	−3.86	8.53	−3.77	12.3
SO_2	12.85	0.5	8.14	−4.21	7.97	−4.38	8.23	−4.12	12.35
H_2O	12.36	−0.26	7.35	−5.27	7.21	−5.41	7.4	−5.22	12.62
HCl	12.42	−0.32	8.11	−4.63	7.89	−4.85	8.13	−4.61	12.74
N_2O	13.48	0.59	8.49	−4.4	8.29	−4.6	8.62	−4.27	12.89
CH_4	13.9	0.3	9.55	−4.05	9.37	−4.23	9.46	−4.14	13.6
CO_2	14.36	0.58	9.14	−4.64	8.95	−4.83	9.28	−4.5	13.78
CO	13.74	−0.27	9.14	−4.87	9	−5.01	9.11	−4.9	14.01
H_2	14.8	−0.63	10.5	−4.93	10.39	−5.04	10.26	−5.17	15.43
N_2	15.28	−0.3	10.39	−5.19	10.26	−5.32	10.41	−5.17	15.58
SF_6	16.22	0.52	10.07	−5.63	9.93	−5.77	10.23	−5.47	15.7
F_2	15.69	−0.01	9.52	−6.18	9.44	−6.26	9.62	−6.08	15.7
HF	15.6	−0.43	9.74	−6.29	9.62	−6.41	9.81	−6.22	16.03
Av.		0.12		−4.52		−4.70		−4.50	
Abs.		0.36		4.52		4.70		4.50	

where x is the standard dimensionless density-gradient argument $x(\mathbf{r})=|\nabla\rho(\mathbf{r})|/\rho^{4/3}(\mathbf{r})$, $a=0.5$, $b=40$. Note, that the potential (2.3) with the positive asymptotics $v_{\mathrm{xc}}(\infty)=I_p+\varepsilon_N$ is equivalent to the potential $v_{\mathrm{xc}}^{\mathrm{BP-GRAC}}(\mathbf{r})-(I_p+\varepsilon_N)$ with the zero asymptotic (here the shift is applied to the total potential), since v_{xc} is defined only up to an arbitrary constant. In fact, this latter potential is presented in Fig. 1, by the construction, (2.3), (2.4) it has the form of $v_{\mathrm{xc}}^{\mathrm{BP}}$ in the bulk region and the proper Coulombic asymptotics $-1/r$, due to its LB component. The ionization potentials I_p required for calculation of $v_{\mathrm{xc}}^{\mathrm{BP-GRAC}}$ are taken from the experiment and they are presented in Table I.

The RESPONSE module of the Amsterdam Density Functional program (ADF2000.02 modified/development version)[20–23] has been used to perform TDDFT calculations of molecular response properties[24] with the SAOP, BP–GRAC, LDA, and GGA potentials and with the ALDA xc kernel. We used the even tempered (ET) basis sets[25,26] of Slater-type orbitals (STOs) consisting of the $1s, 2p, 3d,\ldots$ functions with the orbital exponents $Z=ab^i$, $i=1,\ldots,n$, $b=1.7$. Table II presents the number n of $1s$, $2p$, $3d$, and $4f$ functions for each atom and the a values for the most diffuse functions. These ET basis sets were selected monitoring the quality of results with the number of diffuse functions added to standard ET basis sets. To avoid numerical problems, linear combinations of atomic orbitals have been removed from the basis sets, for which the linear dependence due to the addition of a large number of diffuse functions was detected. The results obtained with the present basis appear to be close to the basis set limit.

The calculated average static polarizability α and hyperpolarizability β are given by (the indices $ab\ldots$ label the Cartesian axes x,y,z):

$$\alpha=\tfrac{1}{3}\sum_a \alpha_{aa}, \tag{2.5}$$

$$\beta=\tfrac{1}{5}\sum_b (\beta_{abb}+\beta_{bab}+\beta_{bba}) \tag{2.6}$$

[in (2.6) a is the dipolar axis], while the anisotropy of the polarizability $\Delta\alpha$ is

$$|\Delta\alpha|^2=\tfrac{1}{2}\sum_{a<b}(\alpha_{aa}-\alpha_{bb})^2. \tag{2.7}$$

The components of the dipole polarizability α_{ab} and hyperpolarizability β_{abc} tensors can be defined through an expansion of the dipole moment μ_a into different orders of the external fields E_b

TABLE II. Even-tempered basis set for the H, C, O, F, Si, P, S, Cl atoms (in parentheses the number n of $1s$, $2p$, $3d$, and $4f$) with the orbital exponent $Z=\alpha\beta^i$, $i=1,\ldots,n$, $\beta=1.7$. The value of α for the most diffuse $1s$, $2p$, $3d$, and $4f$ for each atom is indicated.

Atom	$1s$	$2p$	$3d$	$4f$
H($7s5p4d$)	0.057 513	0.156 109	0.239 461	
C($9s7p5d4f$)	0.078 929	0.108 203	0.202 024	0.395 110
N($9s7p5d4f$)	0.092 674	0.124 531	0.202 024	0.395 110
O($9s7p5d44f$)	0.106 588	0.140 372	0.183 658	0.359 191
F($11s7p5d4f$)	0.042 280	0.157 918	0.183 658	0.359 191
Si($11s9p7d4f$)	0.067 811	0.070 834	0.123 252	0.227 488
P($11s9p7d4f$)	0.071 779	0.075 893	0.133 816	0.239 461
S($11s9p7d4f$)	0.076 097	0.082 302	0.147 902	0.251 434
Cl($11s9p7d4f$)	0.080 357	0.087 446	0.140 859	0.239 461

TABLE III. Static isotropic polarizabilities α (in a.u.).

	SAOP	BP–GRAC	BP	BLYP	LDA	Expt.
H_2	5.63	5.34	5.55	5.78	5.91	5.43
HF	5.40	5.71	6.10	6.47	6.23	5.60
F_2	8.08	8.47	8.75	9.13	8.87	8.38
H_2O	9.45	9.80	10.33	10.95	10.60	9.64
N_2	11.82	11.78	12.06	12.55	12.28	11.74
CO	13.01	13.07	13.38	13.95	13.71	13.08
NH_3	14.21	14.53	15.11	15.94	15.57	14.56
CH_4	17.32	17.03	17.07	17.67	17.71	17.27
HCl	17.99	17.62	18.11	19.13	18.63	17.39
CO_2	16.79	17.39	17.48	18.17	17.74	17.51
N_2O	19.07	19.60	19.70	20.45	19.96	19.70
H_2S	25.72	25.10	25.65	27.03	26.50	24.71
SO_2	24.98	25.69	25.82	26.89	26.20	25.61
C_2H_4	28.09	28.14	28.14	29.31	28.88	27.70
C_2H_6	29.87	29.54	29.45	30.42	30.46	29.61
SF_6	29.00	31.06	31.38	32.27	31.96	30.04
Cl_2	31.56	31.15	31.35	32.74	32.00	30.35
PH_3	31.62	30.75	31.05	32.36	32.27	30.93
SiH_4	32.71	32.02	32.00	32.86	33.69	31.90
OCS	34.18	34.49	34.37	35.83	34.92	33.72
CS_2	56.50	55.98	55.39	57.75	56.28	55.28
Av.%	0.07	0.69	2.40	6.86	5.16	
Abs.%	2.48	1.20	2.59	6.86	5.16	

$$\mu_a = \mu_a(E=0) + \sum_b \alpha_{ab} E^b + \frac{1}{2!} \sum_{bc} \beta_{abc} E^b E^c + \cdots . \tag{2.8}$$

The S_{-4} Cauchy coefficient relates to the frequency dispersion in the average dipole polarizability $\alpha(\omega)$

$$\alpha(\omega) = \alpha(0) + S_{-4}\omega^2 + S_{-6}\omega^4 + \cdots . \tag{2.9}$$

The Cauchy coefficients S_{-2k} are calculated from all oscillator strengths f_i, weighted by an even power of the excitation energies ω_i,

$$S_{-2k} = \sum_i \omega_i^{-2k} f_i . \tag{2.10}$$

The S_{-2} coefficient is equal to the average static polarizability α while the S_0 coefficient should be equal to the number of electrons in the basis set limit.

III. RESULTS OF MOLECULAR RESPONSE CALCULATIONS

A key feature of the SAOP potential mentioned in the Introduction, its more attractive character compared to the LDA and GGA potentials, is illustrated with Table I where the corresponding energies ε_N of the highest occupied molecular orbital (HOMO) are compared with the first VIP I_p. Note, that the rigorous KS theory requires $\varepsilon_N = -I_p$ for potentials with the zero asymptotics $v_{xc}(\infty) = 0$. The LDA and GGA $-\varepsilon_N$ values are substantially smaller than I_p, with the BLYP energies being, as a rule, the smallest ones. The BP error in the fourth column of Table I is, actually, the downward shift $-(I_p + \varepsilon_N)$ in the bulk region (with respect to v_{xc}^{BP}) of the GRAC-corrected potential $v_{xc}^{BP-GRAC}(\mathbf{r}) - (I_p + \varepsilon_N)$ presented in Fig. 1. Its average value for the considered molecules amounts to -4.3 eV. Due to the more attrac-

TABLE IV. Anisotropy of static polarizability $\Delta\alpha$ (in a.u.).

	SAOP	BP–GRAC	BP	BLYP	LDA	Expt.
H_2O	0.84	0.43	0.07	0.18	0.04	0.67
H_2S	0.13	0.42	1.08	1.70	1.17	0.67
HF	1.20	1.09	0.96	0.92	0.93	1.33
HCl	1.80	1.48	1.21	1.01	1.18	1.51
NH_3	1.10	1.94	2.67	3.15	2.83	1.94
CO	3.32	3.40	3.42	3.45	3.29	3.57
N_2	4.78	4.69	4.74	4.78	4.67	4.59
C_2H_4	12.40	11.78	11.61	11.60	11.88	11.40
SO_2	11.95	12.61	12.57	12.81	12.55	13.00
CO_2	12.63	13.20	13.24	13.39	13.35	13.83
Cl_2	16.77	16.41	16.35	16.49	16.44	17.53
Av.%:	−9.55	−9.67	−4.78	6.47	−3.70	
Abs.%:	19.92	−10.67	23.63	34.01	26.65	

TABLE V. S_{-4} Cauchy moments (a.u.).

	SAOP	BP–GRAC	BP	BLYP	LDA	Expt.
HF	11.74	13.01	17.08	20.32	17.88	14.40
F_2	16.29	17.59	20.01	22.48	20.39	17.16[a]
N_2	30.48	30.20	32.99	36.92	34.50	30.11
H_2O	33.00	36.05	45.66	55.03	48.82	35.42
CO	48.71	48.84	53.30	59.38	57.47	48.26
CO_2	44.67	48.94	50.22	55.96	51.96	50.99
CH_4	63.61	62.69	63.93	71.22	69.48	62.41
HCl	74.22	71.50	80.93	96.11	87.02	67.12
NH_3	67.70	74.23	91.03	109.79	97.83	71.44
Cl_2	133.84	133.39	138.65	159.51	145.84	125.8
H_2S	150.31	145.00	161.94	193.58	176.04	138.3
SiH_4	189.42	183.71	185.3	202.1	206.78	178.4
PH_3	211.59	201.68	212.53	243.30	232.06	189.8
Av.%:	−0.05	1.78	13.55	30.93	21.21	
Abs.%:	7.34	3.88	13.79	30.93	21.21	

[a]Coupled cluster linear response result (Ref. 43).

tive character of the SAOP potential, its $-\varepsilon_N$ values are much larger than LDA and GGA ones and they are rather close to I_p. The corresponding SAOP average error is only 0.39 eV. Note, that the same average error of ~ 0.4 eV has been reported in Ref. 27 where the SAOP energies $-\varepsilon_i$ have been used to estimate not only the first, but also other valence ionization potentials I_i for 64 molecules.

Table III compares the average static polarizabilities (2.5) of 21 small molecules at the experimental geometry[28,29] calculated with SAOP, BP–GRAC and the standard LDA and GGA (BP, BLYP) potentials with the experimental α values (expt.).[30–36] The molecules in Table III are placed in the order of increasing polarizability. LDA systematically overestimates α, it has the same average of the relative ($\alpha - \alpha_{\text{exp}}$) and absolute $|\alpha - \alpha_{\text{exp}}|$ errors, which amount to 5%. The performance of GGA appears to depend substantially on the type of functional. BLYP produces worse α values with the larger average error of 7%. On the other hand, BP substantially improves upon LDA, with the average absolute error being reduced to 2.6%. Both BP–GRAC and SAOP definitely improve further upon BP for molecules with smaller polarizabilities at the top of Table III (the only exception is the SAOP α value for H_2, which is slightly worse than the BP one). For molecules with larger polarizabilities the trend is not so uniform. The BP–GRAC average absolute error is further reduced to 1.2%, while the SAOP produces almost the same error of 2.5% as BP. Compared to other potentials, SAOP has the much smaller average α error of only 0.07%. This means that, while LDA and GGAs tend to overestimate α, SAOP lacks this systematic overestimation and its α values are distributed around the experimental ones. Table IV presents the anisotropies (2.7) of the static polarizabilities of 11 molecules. One can see from Table IV that LDA, BLYP, and BP yield similar anisotropies. BP–GRAC improves upon BP, especially for the molecules H_2O and H_2S with small anisotropies, while the results of SAOP for this quantity are somewhat worse than the BP–GRAC ones.

Table V presents the S_{-4} Cauchy coefficients (2.10) for 13 molecules. As in the case of polarizabilities, LDA systematically overestimates the S_{-4} coefficient with an average relative $|S_{-4}|$ error of 21% and BLYP increases further this error. On the other hand, BP improves upon LDA and the BP error is reduced to 14%. Both BP–GRAC and SAOP definitely improve further upon BP, in particular, the BP–GRAC S_{-4} values are better than the BP ones in all cases except CO_2. This brings both SAOP and BP–GRAC $|S_{-4}|$ errors down to 7.3% and 3.9%, respectively (see Table VIII). SAOP produces also a very small average S_{-4} error of only -0.05%.

Table VI compares the average static hyperpolarizabilities β (2.6) of the molecules NH_3, CO, H_2O, and HF calculated with SAOP, BP–GRAC, LDA, and GGA with the *ab initio* ones obtained in Ref. 37 with the coupled cluster CCSD and CCSD(T) methods. Again, LDA produced overestimated values with the average $|\beta|$ error [with respect to CCSD(T)] of 35% and BLYP increases further the error to 41%. In this case, however, BP does not improve substantially upon LDA, the BP β values appear to be rather close to the LDA ones with the average error of 26%. Both SAOP

TABLE VI. Hyperpolarizability $\beta_{\|}$.

	SAOP	BP–GRAC	BP	BLYP	LDA	CCSD	CCSD(T)
NH_3	−33.9	−37.87	−48.4	−56.00	−51.4	−30.0	−34.3
CO	22.18	21.90	28.83	31.8	30.5	23.00	23.5
H_2O	−17.3	−18.2	−22.2	−25.0	−24.6	−16.2	−18.0
HF	−7.2	−7.2	−8.5	−9.3	−9.0	−6.8	−7.3
Abs.%	3.01	4.92	25.9	41.2	34.9		

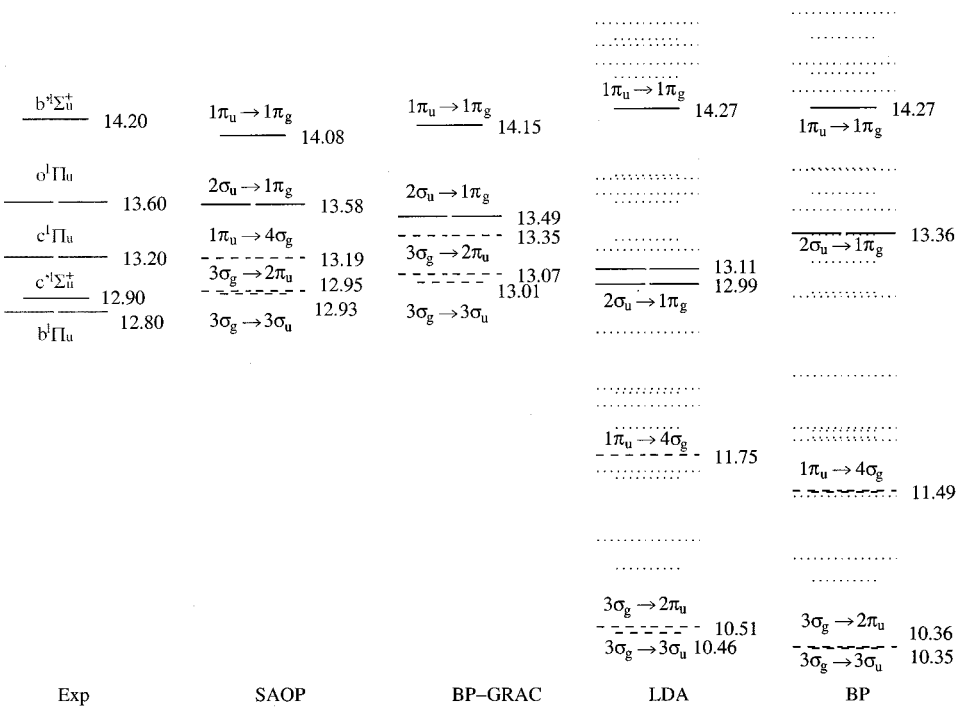

FIG. 2. The experimentally observed (Ref. 38) excited state levels are given to the left. The levels correspond to the Franck–Condon maximum in the absorption. The calculated levels according to the various model Kohn–Sham potentials are given in the other columns. The valence excited states are indicated with drawn lines, and the Rydberg states with broken lines. The many spurious Rydberg states occurring for the LDA and the BP potentials are indicated with dotted lines.

and BP–GRAC improve substantially upon BP, with the average $|\beta|$ error being reduced to 3% and 5%, respectively. Thus, application of the SAOP and BP–GRAC potentials bring the DFT hyperpolarizabilities rather close to those obtained with the most advanced *ab initio* coupled cluster methods. It should be cautioned, however, that at this point the comparison is not definitive, errors in either the CCSD(T) values (due to basis set deficiencies, for instance) or in the SAOP or BP–GRAC values may be as large as their difference.

To sum up, SAOP, BP–GRAC, and BP produce polarizabilities α of the same good quality and they substantially improve upon LDA and BLYP. However, SAOP and BP–GRAC perform definitely better than BP in calculation of the S_{-4} Cauchy coefficients and, especially, in calculation of the hyperpolarizabilities β. These trends will be rationalized in the next section with the spectral analysis of the response properties of the N_2 molecule.

IV. SPECTRAL ANALYSIS OF THE RESPONSE PROPERTIES OF N_2

A physically sound TDDFT approach should reproduce not only total response quantities, such as α and S_{-4}, but also their spectral structure, i.e., the oscillator strenghts f_i and energies ω_i of individual excitations, which determine α and S_{-4} through the sum rules [i.e., particular cases of Eq. (2.10)]

$$\alpha = \sum_i \frac{f_i}{\omega_i^2}, \tag{4.1}$$

$$S_{-4} = \sum_i \frac{f_i}{\omega_i^4}, \tag{4.2}$$

$$N = \sum_i f_i . \tag{4.3}$$

Figure 2 compares the molecular state diagram produced from the experimental data for the five lowest (below 15 eV) dipole allowed excitations of the N_2 molecule[38,39] with the diagrams obtained with the SAOP, BP–GRAC, BP, and LDA potentials. The corresponding excitation energies ω_i are presented in Table VII. There are also presented (in parentheses, below the experimental ω_i values) as representative accurate *ab initio* values the excitation energies obtained recently with the size-consistent self-consistent configuration interaction operator $(SC)^2CI$ applied to the complete active space single and double CI (CAS–SDCI). We note that the experimental spectra exhibit strongly overlapping progressions of vibronic states, which sometimes are perturbed due to interaction. Since we calculate vertical transitions we cite in the table the experimental transition energies to the vibrational states with maximum intensity. These do not always stand out unambigouously, and in view of the vibrational level splittings ranging from 0.1 to 0.25 eV we should take the "experimental" benchmark levels to have an uncertainty of ca. 0.1 eV.

There are two $^1\Sigma_u^+$ states and three $^1\Pi_u$ states. The assignment of the two $^1\Sigma_u^+$ states to $3\sigma_g \rightarrow 3\sigma_u$ and $1\pi_u \rightarrow 1\pi_g$ orbital transitions agrees with what has been inferred from experiment and the SAOP/BP–GRAC energies of these excitations agree perfectly with the corresponding experimental and *ab initio* values. The excitation to the $b'\,^1\Sigma_u^+$ state has valence character $(\pi \rightarrow \pi^*)$, while the $c'\,^1\Sigma_u^+(3\sigma_g \rightarrow 3\sigma_u)$ state is usually referred to as the lowest Rydberg state in N_2 (we indicate valence excited states in Fig. 2 with drawn lines, the Rydberg states with broken lines). This indicates that the $3\sigma_u$ is not simply the expected antibonding combination of $2p\sigma$ AO's on the N atoms (in which case we would be dealing with a valence excitation). Indeed, because of the short N–N distance the $2p\sigma - 2p\sigma$ is extremely antibonding and very high lying, and we find the $3\sigma_u$ to be a very diffuse strongly hybridized (so as to reduce

TABLE VII. The oscillator strengths f, the corresponding excitation energy ω and the assigned orbital transition $\psi_i \rightarrow \psi_a$ for the 5 lowest experimental (expt.) excitations are compared with the f and ω obtained with SAOP, BP–GRAC, and LDA/GGA calculations for these excitations (see Sec. IV for discussion of assignment). Below the experimental excitation energies a representative value from recent very accurate *ab initio* calculations is given; see text. Also, the contributions f/ω^2, f/ω^4 to the polarizability and to the Cauchy coefficient are reported for each excited state as well as their sum over these states.

	SAOP	BP–GRAC	BP	BLYP	LDA	Expt.
$3\sigma_g \rightarrow 3\sigma_u$	98%	98%	100%	100%	100%	$c'\,^1\Sigma_u^+$
ω	12.93	13.01	10.35	10.20	10.46	$\sim$12.9
						(12.83)
f	0.219	0.216	0.003	0.004	0.003	0.279
f/ω^2	0.97	0.95	0.02	0.03	0.02	$\sim$1.24
f/ω^4	4.31	4.14	0.13	0.22	0.13	$\sim$5.76
$3\sigma_g \rightarrow 2\pi_u$	99%	99%	100%	100%	100%	$b\,^1\Pi_u$
ω	12.95	13.07	10.36	10.24	10.51	$\sim$12.8
						(12.86)
f	0.122	0.100	0.004	0.006	0.005	0.243
f/ω^2	0.54	0.44	0.03	0.02	0.04	$\sim$1.10
f/ω^4	2.36	1.86	0.19	0.17	0.24	$\sim$4.97
$1\pi_u \rightarrow 4\sigma_g$	96%	59%	99%	100%	100%	$c\,^1\Pi_u$
ω	13.19	13.35	11.49	11.22	11.75	$\sim$13.2
						(13.45)
f	0.189	0.374	0.013	0.033	0.019	0.145
f/ω^2	0.80	1.54	0.09	0.20	0.15	$\sim$0.63
f/ω^4	3.42	6.44	0.48	1.16	0.84	$\sim$2.47
$2\sigma_u \rightarrow 1\pi_g$	91%	55%	85%	75%(12%)	78%(10%)	$o\,^1\Pi_u$
ω	13.58	13.49	13.36	13.21(13.11)	12.99(13.11)	$\sim$13.6
						(13.52)
f	0.166	0.02	0.292	0.094(0.19)	0.094(0.20)	0.080
f/ω^2	0.67	0.08	1.21	0.40(0.82)	0.41(0.86)	$\sim$0.32
f/ω^4	1.70	0.34	5.02	1.70(3.54)	1.84(3.70)	$\sim$1.28
$1\pi_u \rightarrow 1\pi_g$	59%	58%	26%	26%	22%	$b'\,^1\Sigma_u^+$
ω	14.08	14.15	14.27	14.00	14.27	$\sim$14.2
						(14.33)
f	0.432	0.431	0.245	0.239	0.212	0.278
f/ω^2	1.61	1.59	0.90	0.90	0.77	$\sim$1.03
f/ω^4	6.02	5.98	3.25	3.4	2.81	$\sim$3.81
Σf	1.13	1.14	0.557	0.376(0.566)	0.333(0.533)	1.025
$\Sigma f/\omega^2$	4.60	4.61	2.25	1.55(2.37)	1.39(2.25)	$\sim$4.30
$\Sigma f/\omega^4$	18.82	18.68	9.07	5.65(9.19)	5.86(9.50)	$\sim$18.13

antibonding character) combination of notably atomic $4s$ and $4p$ character. This confirms the experimental assignment of Rydberg character.

As for the three $^1\Pi_u$ states we obtain almost perfect agreement with experiment for both the SAOP and BP–GRAC potentials when we assign the three calculated $^1\Pi_u$ states with $3\sigma_g \rightarrow 2\pi_u$, $1\pi_u \rightarrow 4\sigma_g$, and $2\sigma_u \rightarrow 1\pi_g$ character to the $b\,^1\Pi_u$, $c\,^1\Pi_u$, and $o\,^1\Pi_u$ states, respectively. The SAOP/BP–GRAC ω_i values are very close to the *ab initio* ones for the same type of excitation. This assignment would imply that the highest state of $^1\Pi_u$ symmetry, $o\,^1\Pi_u$, has valence character ($2\sigma_u \rightarrow 1\pi_g$), while the other ones have Rydberg character. However, in the experimental work[39] the $2\sigma_u \rightarrow 1\pi_g$ valence character has been ascribed to the lowest state of $^1\Pi_u$ symmetry, the $b\,^1\Pi_u$. This latter assignment would lead to a discrepancy between experiment and theory in the sense, that SAOP and BP–GRAC as well as the cited $(SC)^2$CAS–SDCI method and other *ab initio* methods[40,41] all overestimate the energy of the valence $2\sigma_u \rightarrow 1\pi_g$ vertical excitation by 0.7–0.8 eV. Furthermore, we have calculated the potential curve for this excited state with SAOP and found that it corresponds better to the curve fitted from the experimental data for the $o\,^1\Pi_u$ state in the sense that it gives similar high vibration frequency. It does not exhibit the considerable softening of the curve that is typical for the lowest excited state, $b\,^1\Pi_u$. It is clear from our potential energy curves that our lowest excitation energies at the various bond distances would indeed correspond to a rather soft vibration, as found in the experiment for $b\,^1\Pi_u$. These lowest excitations change character from $3\sigma_g \rightarrow 2\pi_u$ to $1\pi_u \rightarrow 4\sigma_g$, i.e., the calculated lowest $^1\Pi_u$ state ($b\,^1\Pi_u$) exhibits an avoided crossing with the $c\,^1\Pi_u$. It is clear that further

detailed calculations of the potential curves of all involved $^1\Pi_u$ states with the proper non-Born–Oppenheimer treatment of their vibronic interaction are required to fully resolve the issue of experimental assignment versus theoretical calculations.

Comparing now to the BP and LDA calculations, we note that these produce similar to each other and qualitatively incorrect excitation spectra. First of all, the considered three Rydberg-type states (broken lines in Fig. 2) are shifted downward by 2.2–2.8 eV in the BP and LDA diagrams compared to the experiment. Furthermore, as many as 25 other Rydberg and mixed states (dotted lines in Fig. 2) are placed by BP and LDA below 15 eV. The excitations with valence character ($2\sigma_u \rightarrow 1\pi_g$ and $1\pi_u \rightarrow 1\pi_g$), however, are not shifted much in the LDA/GGA calculations and remain in good agreement with the experimental, SAOP and BP–GRAC $o\,^1\Pi_u$ and $b'\,^1\Sigma_u^+$ states.

The incorrect LDA/GGA spectra are, clearly, artefacts of the deficient LDA/GGA potentials, specifically, of their upward shift in the bulk region displayed in Fig. 1. This shift does not influence valence excitations, since the participating occupied and unoccupied valence orbitals, which are localized in the bulk region, both experience approximately the same upward shift. However, in the outer region the difference between the LDA/GGA and SAOP/BP–GRAC potentials is reduced, since all potentials approach (though in a different way) the zero asymptotics. Because of this, the LDA/GGA upward shift for Rydberg orbitals in the outer region is substantially smaller, than that for valence orbitals in the bulk region. This causes an artificial stabilization of the Rydberg orbitals with respect to the valence ones, which produces the underestimated LDA/GGA energies ω_i of the Rydberg excitations (see Table VII) and, as a result, the incorrect LDA/GGA spectra with many Rydberg-type states below 15 eV presented in Fig. 2.

Besides the excitation energy ω_i, Table VII presents also the oscillator strength f_i and the percentage of the main orbital transition $\psi_i \rightarrow \psi_a$ for each considered excited state, obtained with the SAOP, BP–GRAC, BP, BLYP, and LDA potentials. In the case of the SAOP and BP–GRAC calculations, as well as for the experimental data, we are simply dealing with the five lowest excited states, but for the LDA and GGA potentials we have to identify the appropriate excited states among the many spurious Rydberg states. In almost all cases (with a caveat for $b'\,^1\Sigma_u^+$, see below) it was possible for each of the potentials to unambiguously identify the excited state with the main contribution from a given orbital transition. In the table are also presented individual and overall contributions from the lowest excitations to α and S_{-4}.

We consider, first, the valence excitations $2\sigma_u \rightarrow 1\pi_g$ and $1\pi_u \rightarrow 1\pi_g$ which are associated according to our assignment with the two highest states, $b'\,^1\Sigma_u^+$ and $o\,^1\Pi_u$. The excitation energies of SAOP are in excellent agreement with experiment, as are the oscillator strengths f_i. We note that the oscillator strengths are very difficult to calculate to high accuracy, being very sensitive to small changes in orbital composition of transitions, basis set, etc. Agreement within a factor of 2 with experiment can be considered very satisfactory. The energies of BP–GRAC are also very good, but the $2\sigma_u \rightarrow 1\pi_g$ excitation being a bit low and the next lower $1\pi_u \rightarrow 4\sigma_g$ excitation being a bit high leads to strong mixing between these orbital excitations (almost 50/50). As a result the oscillator strength of the BP–GRAC $2\sigma_u \rightarrow 1\pi_g$ ($o\,^1\Pi_u$) is rather low and that of $1\pi_u \rightarrow 4\sigma_g$ ($c\,^1\Pi_u$) rather high. The contributions from the $2\sigma_u \rightarrow 1\pi_g$ and $1\pi_u \rightarrow 4\sigma_g$ transitions to the f_i partially cancel each other for the former state and they add up for the latter state. Turning to the LDA/GGA calculations, we have already noted that LDA, BP, and BLYP energies ω_i are not very different from the SAOP and BP–GRAC ones and accordingly also reproduce the experimental excitation energies reasonably well. It appears, however, that LDA/GGAs distort seriously the orbital structure of the TDDFT solution for these excitations. Indeed, although the contribution of the valence orbital transition $1\pi_u \rightarrow 1\pi_g$ to the excitation associated with the $b'\,^1\Sigma_u^+$ state is the largest of all contributing orbital transitions, it is only $\sim$25% according to LDA, BLYP, and BP. Many smaller contributions come from numerous Rydberg-type orbital transitions $\psi_i \rightarrow \psi_a$ which, in turn, bring their dominant contributions to the corresponding Rydberg-type states with have energies close to that of the $b'\,^1\Sigma_u^+$ state (see Fig. 2). As for the $o\,^1\Pi_u$ state, although LDA and BLYP still have the orbital transition $2\sigma_u \rightarrow 1\pi_g$ as dominant contribution, they produce also an appreciable contribution of $2\sigma_u \rightarrow 1\pi_g$ to another excitation with the energy 13.1 eV, which is very close to the 12.99 eV they obtain for the $o\,^1\Pi_u$ state. The ω_i and f_i values for this additional excitation are given in parentheses in the corresponding columns of Table VII. This situation, where a strong mixture of the valence and Rydberg orbital transitions occurs because of the presence of a multitude of Rydberg excitations with energies close to the valence excitations, as presented in Fig. 2, occurs for both the $1\pi_u \rightarrow 1\pi_g$ and the $2\sigma_u \rightarrow 1\pi_g$ excitations and creates a serious problem for the proper interpretation of the LDA/GGA TDDFT spectrum. The latter is, clearly, an artifact of the relative stabilization of the Rydberg-type orbitals in the deficient LDA/GGA potentials discussed above.

Note, that the SAOP TDDFT solution for the valence excitations does not present such an interpretation problem. Indeed, with SAOP the excitation associated with the $o\,^1\Pi_u$ state is produced predominantly (91%) with the assigned orbital transition $2\sigma_u \rightarrow 1\pi_g$ (see Table VII). In the other valence excitation associated with the $b'\,^1\Sigma_u^+$ state the assigned orbital transition $1\pi_u \rightarrow 1\pi_g$ is mixed with Rydberg transitions according to both SAOP and BP–GRAC, but these Rydberg orbital transitions are the predominant contributions to Rydberg-type states, which are lying much higher than the $b'\,^1\Sigma_u^+$ state, so that this does not present a problem for the assignment of the SAOP and BP–GRAC spectra.

We proceed our spectral analysis with the discussion of the lowest Rydberg-type excitations in Table VII. In this case for all potentials the assigned orbital transitions bring dominant contributions to the corresponding excitations, with the above-mentioned exception of the contribution of the $1\pi_u \rightarrow 4\sigma_g$ excitation to the $c\,^1\Pi_u$ state for BP–GRAC, where it gets mixed with the valence $2\sigma_u \rightarrow 1\pi_g$. However, there is a remarkable difference between the oscillator strengths f_i cal-

culated for these Rydberg excitations with the SAOP and BP–GRAC potentials, on the one side, and with the LDA, BLYP, and BP potentials, on the other side. LDA/GGAs produce very low f_i, which are much smaller than the experimental values for all three Rydberg-type excitations of Table VII. SAOP and BP–GRAC produce much larger f_i, in particular, for the lowest $3\sigma_g \rightarrow 3\sigma_u$ excitation the SAOP/BP–GRAC f_i are 50–70 times as large and for the next $3\sigma_g \rightarrow 2\pi_u$ excitation they are 20–30 times as large as the LDA/GGA f_i. On the other hand, these SAOP/BP–GRAC f_i are rather close to the experimental values.

The reason for these very different f_i values appears to be the different size of the relevant Rydberg-type molecular orbitals (MOs) calculated with the SAOP/BP–GRAC and with the LDA/GGA potentials. The analysis of these MOs in terms of the atomic orbitals (AOs) of the N atoms reveals that, while the $3\sigma_u$, $2\pi_u$, and $4\sigma_g$ MOs calculated with LDA/GGA consist, predominantly, of the $3s$, $3p$ AOs, the same MOs calculated with SAOP/BP–GRAC consist, mainly, of the substantially more diffuse $4s$, $4p$ and higher lying AOs. The resultant more diffuse SAOP/BP–GRAC $3\sigma_u$, $2\pi_u$, and $4\sigma_g$ MOs yield larger orbital transition moments $r^{\mu}_{ia}=\langle \psi_i | r^{\mu} | \psi_a \rangle$ (r^{μ} is x, y or z) than those calculated with LDA/GGAs. This difference is further amplified for the oscillator strengths f_i, which include the squares of r^{μ}_{ia}.

The physical reason for the different size of the Rydberg-type orbitals obtained with the SAOP/BP–GRAC and LDA/GGA potentials is, again, the deficient form of the latter potentials, this time in the outer region. Indeed, as can be clearly seen from Fig. 1, the LDA/GGA potentials with their fast decay differ appreciably from zero in a much more restricted area than the SAOP and BP–GRAC potentials with their correct Coulombic asymptotics. Because of this, the former potentials confine bound Rydberg MOs in the restricted area, making them more localized, while the latter potentials support more diffuse Rydberg MOs. These more diffuse MOs produce much larger SAOP/BP–GRAC oscillator strengths f_i, as was explained above.

The above-mentioned low f_i for the three Rydberg-type excitations make partial LDA/GGA sums $\Sigma_i f_i$ over our five states in Table VII much smaller compared to the experimental ones. The sums calculated with LDA and BLYP are especially low, but if we add (in parentheses in the corresponding columns of Table VII) the additional excitation with an appreciable contribution from the $2\sigma_u \rightarrow 1\pi_g$ orbital transition (see the discussion above), the LDA and BLYP sums become close to the BP one. The factors by which the f_i, which are in the numerators of (4.1) and (4.2), are too low are more significant than the too large factors $1/\omega_i^2$ and $1/\omega_i^4$ due to the smaller energies ω_i in the denominators, thus producing low LDA/GGA partial α and S_{-4} values, which are 2 to 3 times smaller than the corresponding experimental values. In contrast, the SAOP and BP–GRAC overall pictures for the lowest dipole allowed excitations agree very well with the experiment. SAOP and BP–GRAC yield practically the same partial f sums, which are close to the experimental estimate and, as was discussed above, they reproduce the experimental excitation energies ω_i. As a result, the SAOP and BP–GRAC partial α and S_{-4} values appear to be close to each other and to the experimental values (see Table VII).

Interesting enough, the above-mentioned LDA/GGA underestimation of the contributions from the lowest excitations is more than compensated with overestimated contributions from higher excitations, the summation over which (to obtain α and S_{-4}) is supposed to represent integration (in a Stieltjes sense) over the underlying ionization continuum. Table VIII presents the f_i and ω_i values calculated for excitations with energies ω_i, which are higher than the N_2 ionization energy $I_p=15.6$ eV and lower than the threshold of 22 eV, and which have oscillator strengths f_i higher than 0.1. Just as in Table VII, the LDA/GGA energies ω_i of Table VIII are consistently lower than the SAOP and BP–GRAC ones. However, unlike in Table VII, the LDA/GGA oscillator strengths f_i for the excitations in Table VIII appear to be systematically larger than the SAOP/BP–GRAC ones. This latter trend can be understood qualitatively from the sum rule (4.3), which requires the sum over f_i to be the constant N, the total number of electrons. Then, underestimation of the partial sum $\Sigma_i f_i$ over the lowest excitations in Table VII must be compensated with a corresponding overestimation for higher excitations, which can be seen from Table VIII. In this latter case, the LDA/GGA underestimation of ω_i and overestimation of f_i work in the same direction, so that the LDA/GGA partial α and S_{-4} values for the ''continuum'' states are substantially larger than the SAOP/BP–GRAC ones (see Table VIII).

Thus, BP as well as LDA and BLYP substantially underestimate contributions to α and S_{-4} from the Rydberg-state excitations and they overestimate those from the ''continuum'' states. Contrary to this, SAOP and BP–GRAC yield a more balanced ''excitation structure'' of α and S_{-4}, which is remarkably similar for both methods and which agrees well with the experimental data for the lowest excitations. Due to the partial compensation of the above-mentioned LDA/GGA errors of opposite signs, the total LDA/GGA polarizabilities for N_2 are in better agreement with experiment than the corresponding partial sums over the lowest excitations (compare Tables III and VII). An especially lucky error compensation occurs for BP with $\alpha=12.06$ a.u., which is not much larger than the experimental value $\alpha=11.74$ a.u., though the SAOP $\alpha=11.82$ a.u. and BP–GRAC $\alpha=11.78$ a.u. still have smaller errors. Then, bearing in mind that BP underestimates the higher excitation energies ω_i and that the S_{-4} sum (4.2) has the additional ω_i^2 factor in the denominator compared to the α sum (4.1), one can expect a larger BP overestimation for the S_{-4} Cauchy coefficient. Indeed, as follows from Table V, the BP value $S_{-4}=32.99$ a.u. is appreciably larger than the experimental $S_{-4}=30.11$ a.u., while the SAOP $S_{-4}=30.48$ a.u. and the BP–GRAC $S_{-4}=30.20$ a.u. are close to the experiment.

The spectral analysis of the polarizability α and the S_{-4} Cauchy coefficient of N_2 performed in this section shows, that LDA and GGAs all produce a distorted picture of the contributions to α and S_{-4} from individual excitations. In contrast, SAOP and BP–GRAC both yield a qualitatively correct structure of α and S_{-4}. General conclusions from this analysis will be drawn in the next section.

TABLE VIII. Oscillator strength f and excitation energy ω calculated for the excitations which have energies higher than the N_2 ionization potential and lower than 22 eV and oscillator strengths larger than 0.1. The contributions f/ω^2, f/ω^4 to the polarizability and to the Cauchy coefficient are reported, as well as their sums over these states.

	SAOP	BP–GRAC	BP	BLYP	LDA
$1\pi_u \rightarrow 2\delta_g$	96%	94%	94%	87%	87%
ω	17.06	17.16	14.59	14.20	14.73
f	0.113	0.140	0.16	0.20	0.154
f/ω^2	0.28	0.35	0.56	0.76	0.52
f/ω^4	0.72	0.88	1.94	2.76	1.80
$3\sigma_g \rightarrow 8\sigma_u$	100%	100%	99%	99%	99%
ω	17.64	17.58	15.20	14.85	15.19
f	0.142	0.132	0.167	0.148	0.160
f/ω^2	0.34	0.32	0.54	0.50	0.51
f/ω^4	0.81	0.75	1.72	1.66	1.65
$1\pi_u \rightarrow 11\sigma_g$	96%	97%	99%	99%	99%
ω	20.36	20.44	18.69	18.33	18.78
f	0.100	0.109	0.174	0.160	0.160
f/ω^2	0.18	0.19	0.36	0.36	0.34
f/ω^4	0.32	0.34	0.78	0.80	0.70
$1\pi_u \rightarrow 4\delta_g$	91%	80%	94%	95%	94%
ω	21.54	21.65	20.55	20.13	20.55
f	0.704	0.600	0.84	0.82	0.80
f/ω^2	1.12	0.94	1.48	1.50	1.42
f/ω^4	1.80	1.50	2.60	2.76	2.48
Σf	1.059	0.981	1.341	1.328	1.274
$\Sigma f/\omega^2$	1.92	1.90	2.94	3.12	2.79
$\Sigma f/\omega^4$	3.65	3.47	7.04	7.98	6.63

V. CONCLUSIONS

It has often been observed that in particular excitations to Rydberg states are affected by the shape corrections to the LDA and GGA xc potentials, while valence excitations are believed to be represented reasonably well by LDA and GGA calculations. In this paper the performance of the approximate SAOP[7] and BP-GRAC[8] xc potentials has been assessed in molecular TDDFT calculations of the static average polarizability α, and its frequency dispersion in the form of the S_{-4} Cauchy coefficient, and the static average hyperpolarizability β. The results have been compared with those obtained with the standard LDA and some GGA (BP and BLYP) potentials, and the performance of these potentials has been more closely examined by explicitly considering the spectral structure of α and S_{-4}.

Due to their correct form, the SAOP and BP–GRAC potentials reproduce well the characteristics of the molecular excitation spectra, such as individual excitation energies ω_i and oscillator strengths f_i. In contrast, standard LDA and GGA potentials produce a distorted spectral structure of α and S_{-4}. They tend to underestimate the energies ω_i and they also appear to underestimate the oscillator strengths f_i of excitations to bound Rydberg-type states and overestimate those for excitations to the ''continuum'' states. As a result, LDA and GGAs tend to underestimate contributions to α and S_{-4} from Rydberg-type states and to overestimate those from the continuum, so that these errors of opposite signs partially compensate each other.

These distortions of the LDA/GGA spectra have been related to the deficient form of the corresponding potentials in both bulk and outer regions. In particular, artificial stabilization (low energies ω_i) of the Rydberg-type states is due to the upward shift of the LDA/GGA potentials in the bulk region. In turn, artificial localization of bound Rydberg-type states, which results in low oscillator strengths f_i, is due to the fast decay of the LDA/GGA potentials in the outer region, which makes the LDA/GGA potential well considerably more narrow than the asymptotically corrected SAOP and BP–GRAC potentials, see Fig. 1. The distortions create a serious problem for the assignment of the LDA/GGA TDDFT spectra. The SAOP and BP–GRAC potentials, which are free from the above-mentioned deficiencies, produce a balanced spectral structure of the molecular response quantities.

Both SAOP and BP–GRAC yield high quality molecular polarizabilities α, Cauchy coefficients S_{-4}, and hyperpolarizabilities β for the considered molecules. The SAOP and BP–GRAC average errors for these properties are only a few percent and they improve substantially upon LDA and BLYP. Due to somewhat reduced errors from individual excitations and their lucky cancellation, BP also reproduces well the polarizabilities. However, the distorted BP spectral structure of the response properties manifests itself in a worsening quality of the BP Cauchy coefficients and hyperpolarizabilities.

Further refinement of the SAOP and BP–GRAC potentials can further enhance the quality of the TDDFT results. Within SAOP, for example, one can apply statistical averag-

ing separately to the xc hole and "response" [42] parts of a model xc potential. Within the GRAC procedure, one can use, instead of the BP potential, the derivative of an exchange-correlation energy functional with parameters which would be directly fitted to reproduce molecular response properties calculated with the resultant GRAC potential. Further improvement of the TDDFT results might also require (especially for larger, more polarizable molecules) refinement of the xc kernel beyond the ALDA f_{xc} employed in the present paper.

[1] R. van Leeuwen and E. J. Baerends, Phys. Rev. A **49**, 2421 (1994).
[2] S. J. A. van Gisbergen, V. P. Osinga, O. V. Gritsenko, R. van Leeuwen, J. G. Snijders, and E. J. Baerends, J. Chem. Phys. **105**, 3142 (1996).
[3] M. E. Casida, K. C. Casida, and D. R. Salahub, Int. J. Quantum Chem. **70**, 933 (1998).
[4] D. J. Tozer and N. C. Handy, J. Chem. Phys. **109**, 10180 (1998).
[5] S. J. A. van Gisbergen, F. Koostra, P. R. T. Schipper, O. V. Gritsenko, J. G. Snijders, and E. J. Baerends, Phys. Rev. A **57**, 2556 (1998).
[6] M. E. Casida and D. R. Salahub, J. Chem. Phys. **113**, 8918 (2000).
[7] P. R. T. Schipper, O. V. Gritsenko, S. J. A. van Gisbergen, and E. J. Baerends, J. Chem. Phys. **112**, 1344 (2000).
[8] M. Grüning, O. V. Gritsenko, S. J. A. van Gisbergen, and E. J. Baerends, J. Chem. Phys. **114**, 652 (2001).
[9] O. V. Gritsenko, P. R. T. Schipper, and E. J. Baerends, Chem. Phys. Lett. **302**, 199 (1999).
[10] O. V. Gritsenko, P. R. T. Schipper, and E. J. Baerends, Int. J. Quantum Chem. **76**, 407 (2000).
[11] A. Becke, Phys. Rev. A **38**, 3098 (1988).
[12] J. P. Perdew, Phys. Rev. B **33**, 8822 (1986); **34**, 7406(E) (1986).
[13] G. Ricciardi, A. Rosa, and E. J. Baerends, J. Phys. Chem. A **105**, 5242 (2001).
[14] A. Rosa, G. Ricciardi, E. J. Baerends, and S. J. A. van Gisbergen, J. Phys. Chem. A **105**, 3311 (2001).
[15] S. J. A. van Gisbergen, J. M. Pacheco, and E. J. Baerends, Phys. Rev. A **63**, 063201 (2001).
[16] W. Hieringer, S. J. A. van Gisbergen, and E. J. Baerends (unpublished).
[17] M. Petersilka, U. J. Gossmann, and E. K. U. Gross, *Electronic Density Functional Theory: Recent Progress and New Directions* (Plenum, New York, 1998).
[18] C. Lee, W. Yang, and R. G. Parr, Phys. Rev. B **37**, 785 (1988).
[19] O. V. Gritsenko, R. van Leeuwen, E. van Lenthe, and E. J. Baerends, Phys. Rev. A **51**, 1944 (1995).
[20] E. J. Baerends, D. E. Ellis, and P. Ros, Chem. Phys. **2**, 41 (1973).
[21] L. Versluis and T. Ziegler, J. Chem. Phys. **88**, 322 (1988).
[22] G. te Velde and E. J. Baerends, J. Comput. Phys. **99**, 84 (1992).
[23] C. Fonseca Guerra, J. G. Snijders, G. te Velde, and E. J. Baerends, Theor. Chem. Acc. **99**, 391 (1998).
[24] S. J. A. van Gisbergen, J. G. Snijders, and E. J. Baerends, Comput. Phys. Commun. **118**, 119 (1999).
[25] R. C. Raffenetti, J. Chem. Phys. **59**, 5936 (1973).
[26] J. Kobus, D. Moncrieff, and S. Wilson, J. Phys. B **34**, 5127 (2001).
[27] D. P. Chong, O. V. Gritsenko, and E. J. Baerends, J. Chem. Phys. **116**, 1760 (2002).
[28] Landolt-Börstein, *Numerical Data and Functional Relationship in Science and Technology, Group II* (Springer, Berlin, 1992).
[29] K. P. Huber and G. Herzberg, *Constants of Diatomic Molecules* (Van Nostrand-Reinhold, New York, 1979).
[30] T. N. Olney, N. M. Cann, G. Cooper, and C. E. Brion, Chem. Phys. **223**, 59 (1997).
[31] G. D. Zeiss and W. J. Meath, Mol. Phys. **33**, 1155 (1977).
[32] B. L. Jhanwar, W. J. Meath, and J. C. F. McDonald, Can. J. Phys. **59**, 185 (1981).
[33] M. A. Spackman, J. Chem. Phys. **94**, 1288 (1991).
[34] A. J. Russel and M. A. Spackman, Mol. Phys. **90**, 251 (1997).
[35] A. J. Russel and M. A. Spackman, Mol. Phys. **98**, 633 (2000).
[36] J. Dougherty and M. A. Spackman, Mol. Phys. **82**, 193 (1994).
[37] H. Sekino and R. J. Bartlett, J. Chem. Phys. **98**, 3022 (1993).
[38] J. Geiger and B. Schröder, J. Chem. Phys. **50**, 7 (1969).
[39] W. F. Chan, G. Cooper, R. N. S. Sodhi, and C. E. Brion, Chem. Phys. **170**, 81 (1993).
[40] D. C. Comeau and R. J. Bartlett, Chem. Phys. Lett. **207**, 414 (1993).
[41] J. Pitarch-Ruiz, J. Sanchez-Marin, I. Nebot-Gil, and N. Ben Amor, Chem. Phys. Lett. **291**, 407 (1998).
[42] E. J. Baerends and O. V. Gritsenko, J. Phys. Chem. A **101**, 5383 (1997).
[43] E. K. Dalskov and S. P. A. Sauer, J. Phys. Chem. **102**, 5269 (1998).